Biomech Model Mechanobiol (2014) 13:827–838
DOI 10.1007/s10237-013-0537-5

ORIGINAL PAPER

Bone remodelling of the scapula after a total shoulder arthroplasty

C. Quental · P. R. Fernandes · J. Monteiro · J. Folgado

Received: 19 February 2013 / Accepted: 11 October 2013 / Published online: 25 October 2013

Abstract According to Wolff's law, the changes in stress after a prosthesis implantation may modify the shape and internal structure of bone, thus compromising the long-term prosthesis fixation and, consequently, be a significant factor for glenoid loosening. The aim of the present study is to evaluate the changes in the bone adaptation process of the scapula after an anatomical and reverse total shoulder arthroplasty. Five finite element models of the implanted scapula are developed considering the implantation of three anatomical, cemented, all-polyethylene components; an anatomical, cementless, metal-backed component; and a reverse, all-metal component. The methodology followed to simulate the bone adaptation of the scapula was previously validated for the intact model, prior to the prosthesis implantation. Additionally, the influence of the bone quality on the adaptation process is also investigated by considering an osteoporotic condition. The results show that the stress shielding phenomenon is more concerning in cementless, metal-based components than in cemented, all-polyethylene components, regardless of the bone quality. Consequently, as far as the bone adaptation process of the bone is concerned, cemented, all-polyethylene components are better suited for the treatment of the shoulder joint.

Keywords Finite element method · Bone remodelling · Stress shielding · Total shoulder arthroplasty · Glenoid

Electronic supplementary material The online version of this article (doi:10.1007/s10237-013-0537-5) contains supplementary material, which is available to authorized users.

C. Quental · P. R. Fernandes · J. Folgado (✉)
IDMEC, Instituto Superior Técnico, University of Lisbon,
Av. Rovisco Pais, 1049-001 Lisbon, Portugal
e-mail: jfolgado@dem.ist.utl.pt

C. Quental
e-mail: cquental@dem.ist.utl.pt

P. R. Fernandes
e-mail: pfernan@dem.ist.utl.pt

J. Monteiro
Faculty of Medicine, University of Lisbon, Lisbon, Portugal
e-mail: jac.monteiro@hsm.min-saude.pt

1 Introduction

The replacement of the shoulder joint by an implant, known as total shoulder arthroplasty (TSA), has become a common procedure to restore shoulder function and reduce pain. However, although short- and mid-term outcomes of the TSA are satisfactory, there are still significant long-term complications that compromise the procedure. The most concerning complication is aseptic loosening, particularly of the glenoid component (Bohsali et al. 2006; Fealy et al. 2008; Farshad and Gerber 2010), which has a multifactorial aetiology, not yet fully understood (Sundfeldt et al. 2006; Fealy et al. 2008). Among other mechanisms of loosening, the adaptation of bone to the implant is often mentioned as an important element in studies of the hip and knee joints (Bono et al. 2005; Sundfeldt et al. 2006; Fraldi et al. 2010). Under normal, and healthy, conditions, bones support joint and muscle loads by themselves. However, when an implant is introduced into the bone, the loading condition, initially supported by the bone alone, is then shared with the implant. As a result, the bone may be shielded from its normal mechanical stresses, a phenomenon commonly known as stress shielding (Huiskes 1993; Gefen 2002; Poitout 2004), which, based on Wollf's law (Fernandes et al. 1999; Christen et al. 2012), may cause an adverse bone adaptation that threatens the long-term fixation of the implant (Suárez et al. 2012). Furthermore, some studies suggest that the bone loss due to stress shielding may

facilitate bone osteolysis, one of the most concerning mechanisms of loosening in the shoulder arthroplasty, by exposing the bone interfaces to wear particles (Sundfeldt et al. 2006). The loss of bone stock also adds difficulty to the revision of the implant, if, for whatever reason, it is necessary (Nagels et al. 2003). Even though this adaptation process has been extensively studied in the hip and knee arthroplasty, it has received little attention in the shoulder (Pelletier et al. 2008). Consequently, its clinical relevance to the outcome of a TSA is still poorly known (Suárez et al. 2012).

Some numerical studies have already suggested the occurrence of bone adaptation around glenoid prostheses (Stone et al. 1999; Lacroix et al. 2000; Ahir et al. 2004; Gupta et al. 2004a,b; Sharma et al. 2010; Suárez et al. 2012). However, most of these studies based their predictions on stress simulations only, i.e. they did not consider any bone remodelling model, and thus did not explicitly model the adaptation of the bone to the implant (Stone et al. 1999; Lacroix et al. 2000; Ahir et al. 2004; Gupta et al. 2004a,b). The studies of Sharma et al. (2010) and Suárez et al. (2012) are the only ones in which a bone remodelling model was applied. Hence, there is considerably little material addressing the bone adaptation of the scapula following a total shoulder arthroplasty, especially if it is taken into account that only the work of Suárez et al. (2012) combined the complexity of a bone remodelling model and the 3D geometry of a scapula. Note that Sharma et al. (2010) studied the effect of conceptual glenoid prostheses on the bone adaptation of the scapula using 2D finite element models. Furthermore, it is worth noting that only a cementless, metal-backed component was evaluated by Suárez et al. (2012).

In the light of the above, the aim of this study is to evaluate the bone remodelling process due to stress shielding around cemented and cementless glenoid prostheses, and gain further insight into its contribution to the outcome of the TSA. For that purpose, 3D finite element models of the scapula, simulating the idealized immediate condition after the replacement of the shoulder joint by 5 different shoulder prostheses, are developed. The considered prostheses include three anatomical, cemented, all-polyethylene components, with pegged, anchor pegged, and keeled anchorage systems; one anatomical, cementless, metal-backed component; and one reverse, cementless, all-metal component. The bone remodelling simulations are performed having as basis the study conducted previously for an intact, healthy scapula (Quental et al. 2013a). In addition to the bone remodelling parameters deemed before as best to reproduce the actual bone density distribution of the scapula under analysis (Quental et al. 2013a), another set of parameters is also considered here to simulate the behaviour of an osteoporotic bone (Santos et al. 2010). Note that the 3D model of the scapula considered is based on the CT images of a 38-year-old subject with no known health problems, but the replacement of the shoulder joint is primarily performed in the elderly (Hasan et al. 2002; Rasmussen et al. 2012), whose bone stock is generally poorer, in quality and quantity. The impact of each implant on the bone adaptation process of the scapula is assessed by the changes in bone density over time.

2 Methods

2.1 Finite element model

The 3D geometric model of the intact scapula, constructed in Quental et al. (2013a) from the CT images of the Visible Human Project (Spitzer et al. 1996), served as basis for the finite element models developed here. Using this model, the replacement of the shoulder joint was virtually simulated in Solidworks® for 5 designs of shoulder prostheses, being the implant positioning approved by an orthopaedic surgeon. The shoulder implants considered include 3 cemented and 2 cementless glenoid components, whose detailed geometry is provided in Online Resource 1. The cemented components, based on the designs of the Depuy Orthopaedics, are anatomical, all-polyethylene components that either have a pegged, an anchor pegged, or a keeled anchorage system, as depicted in Fig. 1. A uniformly distributed cement mantle of 1 mm was considered around the implants (Terrier et al. 2005). The cementless components, shown in Fig. 2, include (1) an anatomical component, based on the design of the Lima Corporate, which consists of a metal back with a porous coating made of titanium alloy, a polyethylene inlay, and a central screw and two peripheral screws for fixation and (2) a reverse component, based on the DELTA® design of the Depuy Orthopaedics, consisting of a metaglene with a porous coating made of titanium alloy, a 38-mm glenosphere made of cobalt–chromium–molybdenum (CoCrMo) alloy, and a

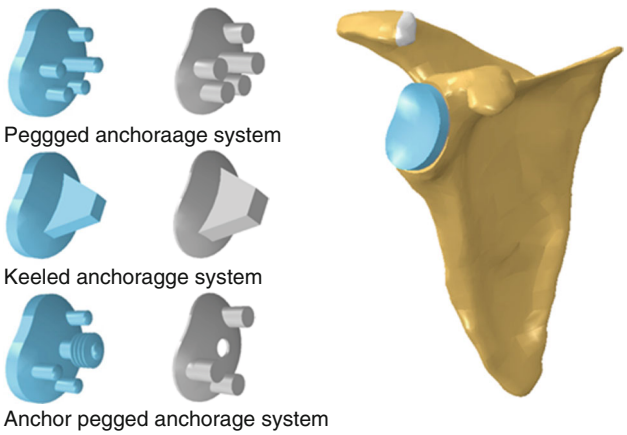

Fig. 1 Finite element models of the cemented glenoid components. The polyethylene components are placed at the most left of the figure, and the corresponding cement mantles are placed next to them

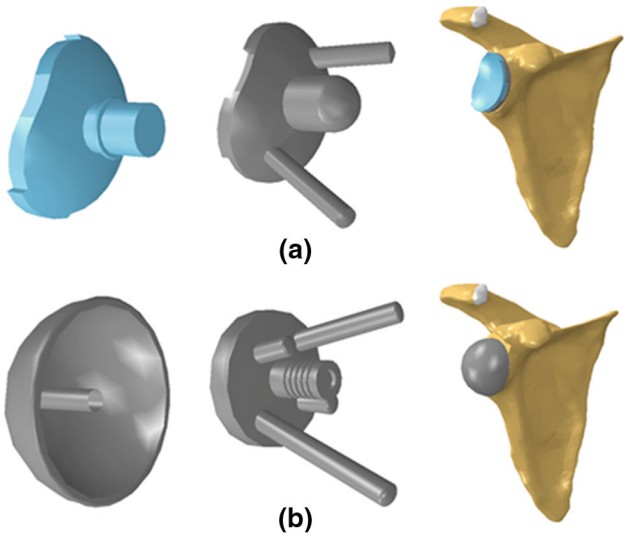

Fig. 2 Finite element models of the cementless glenoid components. The anatomical glenoid component is represented in (**a**), whereas the reverse glenoid component is represented in (**b**). The components placed at the most *left* are made of polyethylene and CoCrMo, from superior to inferior, respectively, and the remaining components are made of titanium

Table 1 Material properties of the glenoid components of the shoulder prostheses and cartilage

Material	Young's modulus (MPa)	Poisson's ratio
CoCrMo (Ahir et al. 2004)	220,000	0.30
Titanium (Ahir et al. 2004)	110,000	0.30
Bone cement (Hopkins et al. 2005)	2,000	0.23
Polyethylene (Hopkins et al. 2005)	500	0.40
Cartilage (Carter and Wong 2003)	6	0.47

central screw and four peripheral screws for fixation. The metaglene was positioned without any inferior tilting, and the length and orientation of the peripheral screws were chosen to maximize the contact between these and the bone, while avoiding their protrusion beyond the scapula boundaries.

The 3D meshes of the described structures were generated in Abaqus® 6.10 using linear tetrahedral elements. All interfaces, bone–cement, cement–implant, and bone–implant, were considered perfectly bonded, simulating an idealized immediate post-operative condition (Hopkins et al. 2005; Terrier et al. 2009).

Apart from polyethylene, which was modelled as an elastic–plastic material using the true stress–strain data presented by Godest et al. (2002), all structures were modelled as linearly elastic materials. The Young's moduli and Poisson's ratios considered are summarized in Table 1. The material properties of bone result from the bone remodelling process assuming a Poisson's ratio of 0.3 and a Young's modulus of 17 GPa for dense compact bone.

2.2 Bone remodelling process

The bone remodelling model applied here was developed by Fernandes et al. (1999). The model considers bone as a linearly elastic orthotropic material obtained by the periodic repetition of a cubic cell with rectangular holes with dimensions a_1, a_2, a_3 (Folgado et al. 2004). At each point, bone is characterized by the parameters $\mathbf{a}$, which are related to bone density, and the Euler angles $\boldsymbol{\theta}$, which define the cubic cell orientation. The relative density μ of bone is given by $1-a_1a_2-a_1a_3-a_2a_3+2a_1a_2a_3$, with a_i bounded between 0 and 1. Mathematically, the bone remodelling process is addressed as the minimization of the structural compliance, i.e. the inverse of the structural stiffness, while taking into account a biological criterion regarding the cost of bone maintenance. The bone remodelling law is stated as

$$\sum_{P=1}^{NC}\left(\alpha^P \frac{\partial E^H_{ijkl}}{\partial \mathbf{a}} e_{kl}\left(\mathbf{u}^P\right) e_{ij}\left(\mathbf{u}^P\right)\right) - \kappa \frac{\partial \mu^m}{\partial \mathbf{a}} = 0 \qquad (1)$$

where NC is the number of applied load cases, α^P are the load weight factors, E^H_{ijkl} are the homogenized bone material properties (Guedes and Kikuchi 1990), e_{ij} and e_{kl} are the components of the strain field, and $\mathbf{u}^P$ is the set of displacements fields computed through the finite element method. The bone remodelling parameters κ and m define the cost of bone maintenance and therefore control the total amount of bone mass.

The bone remodelling model described was successfully validated for the healthy condition of the scapula in Quental et al. (2013a). Ergo, the bone adaptation process of the scapula after TSA, was simulated in this study following a similar methodology, i.e. the bone remodelling law was evaluated at the nodes, and the same twelve load cases, including muscle and joint reaction forces at 10°, 30°, 50°, 70°, 90°, and 110° of arm abduction in the frontal plane and anterior flexion in the sagittal plane, were considered. The corresponding weighting factors α^P are shown in Table 2.

For the models of the anatomical shoulder prostheses, the muscle and joint reaction forces were determined using the detailed musculoskeletal model of the upper limb presented in Quental et al. (2012b, 2013b), which is based on the same subject whose scapula is here analysed. The musculoskeletal model includes 7 rigid bodies, constrained by 6 anatomical joints, and acted upon by 21 muscles of the upper limb. For the model of the reverse shoulder prosthesis, a modified musculoskeletal model of the upper limb, which takes into account the changes in the shoulder joint geometry and position resulting from the reverse TSA, was applied (Quental et al. 2013c). Considering that the primary indication for reverse TSA is total or partial deficiency of the rotator cuff, the supraspinatus, infraspinatus, and subscapu-

Table 2 Load weight factors for the 12 load cases considered

Motion	Arm amplitude					
	10°	30°	50°	70°	90°	110°
Abduction	0.145735	0.069027	0.064054	0.031480	0.006265	0.001621
Flexion	0.312289	0.147916	0.137258	0.067456	0.013425	0.003474

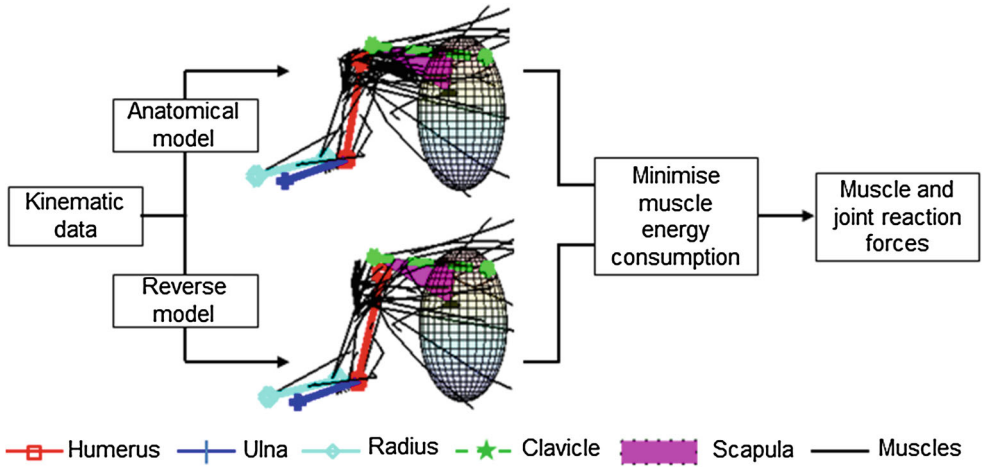

Fig. 3 Schematic of the inverse dynamics procedure applied to estimate the muscle and joint reaction forces of the *upper limb*

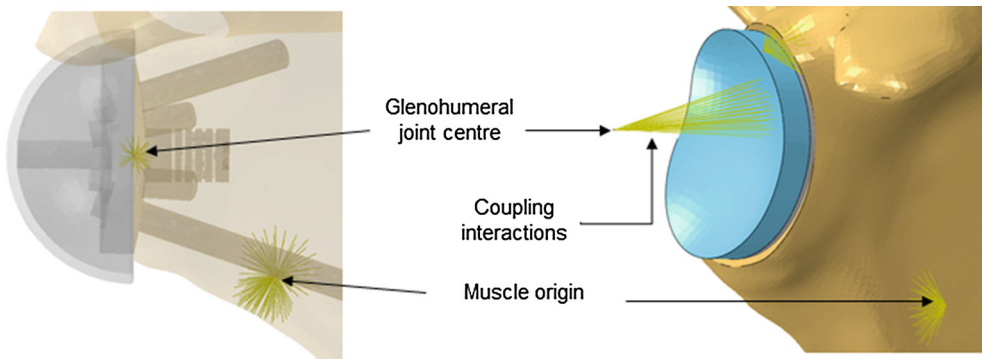

Fig. 4 Coupling interactions considered for the loading condition of the scapula

laris muscles, which are the most commonly affected muscles, were considered inactive (Matava et al. 2005; Melis et al. 2011). The inverse dynamics procedure applied to estimate the muscle and joint reaction forces is schematically represented in Fig. 3. The application point, magnitude, and orientation of the forces estimated are provided in Online Resource 2. In Abaqus, force application points were defined as attachment points, which do not belong to any particular mesh, but are able to transmit force through the definition of coupling constraints, as exemplified in Fig. 4. In order to avoid high punctual stresses, each attachment point was coupled with at least 30 nodes. To avoid rigid body motion, instead of applying the estimated scapulothoracic joint reaction forces, several nodes in the vicinity of the articulation were constrained in all directions (Terrier et al. 2005).

The effect of the implants on the bone adaptation process was evaluated for two conditions of bone: a healthy and an osteoporotic. For the healthy condition, the bone remodelling model was applied using parameters κ and m of 4.00×10^{-4} and 5, respectively, which were deemed as best to reproduce the actual bone density distribution of the modelled scapula (Quental et al. 2013a). The osteoporotic condition was simulated considering a superior cost of bone maintenance. Based on the study of Santos et al. (2010), parameter k was defined 4.7 times greater than that of the healthy condition. Accordingly, a parameter κ of 1.88×10^{-3} and a parameter m of 5 were considered. Note that, for each condition, a bone remodelling analysis of the intact scapula, prior to the prosthesis implantation, was performed to define the initial density distribution of the bone to be considered for the bone remodelling simulations after TSA.

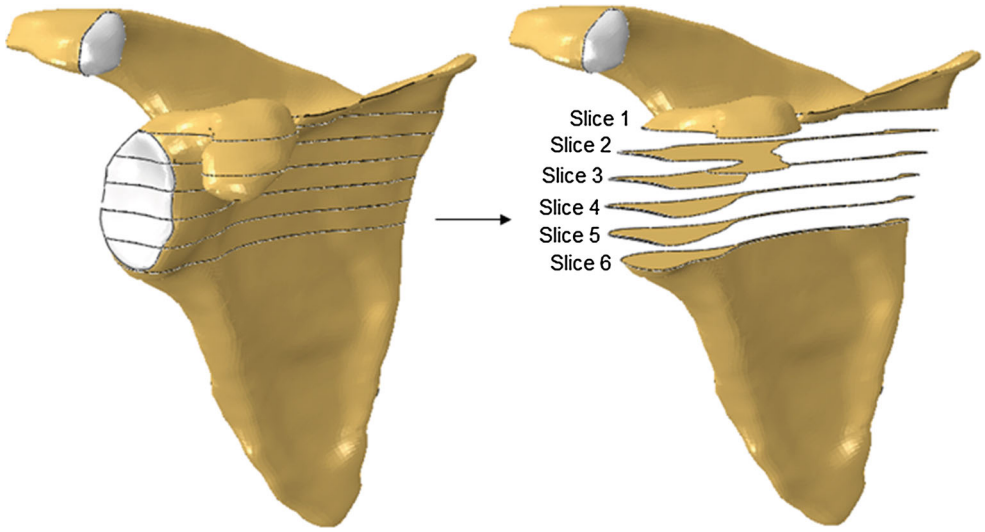

Fig. 5 Slices of the scapula selected for the evaluation of the relative change in bone density

All simulations were terminated when the absolute difference in bone density did not change more than 4×10^{-5} g/cc per node. Mathematically, this criterion is expressed as

$$\frac{1}{n}\sum_{i=1}^{n}|\Delta\rho_i| \leq 4 \times 10^{-5} \tag{2}$$

where n is the number of nodes of the scapula and $\Delta\rho_i$ is the difference in bone apparent density, of node i, between consecutive iterations. Assuming a maximum bone apparent density of 1.8 g/cc for cortical bone (Gupta et al. 2004a,b; Sharma et al. 2010), the bone apparent density ρ_i of node i is related to the relative density μ_i through the expression $\rho_i\,(g/cc) = 1.8 \times \mu_i$.

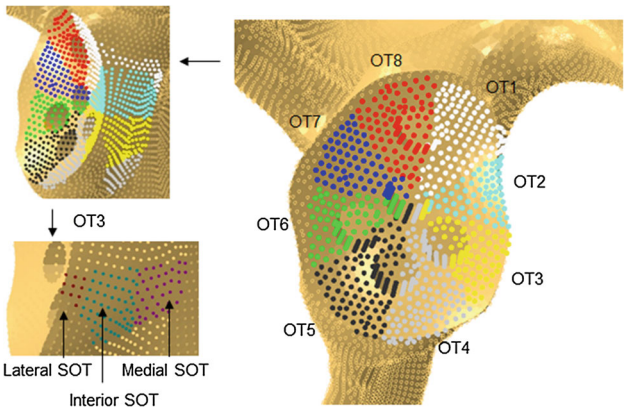

Fig. 6 Division of the glenoid into octants (OT) and sub-octants (SOT). Note that only the nodes at the surface are visible

2.3 Evaluation of the results

In order to evaluate the effect of the glenoid prostheses on the bone adaptation process of the scapula, the difference in bone density, between the predicted results and the initial solution, before the prosthesis implantation, is given for the slices of the glenoid identified in Fig. 5.

Seeking a more quantitative analysis, the glenoid was also divided into 8 octants (OT), and sub-octants (SOT), for which the change in bone mass is provided. The octants divide the glenoid into superior–inferior and anterior–posterior sections, being comprised of all nodes within the volume bounded between the outer surface of the glenoid and the plane parallel to the glenoid that passes few millimetres away, in the medial direction, from the last node of the scapula in contact with the shoulder prosthesis. The sub-octants divide each of the 8 octants into 3 equally distanced sections, defined from the most lateral to the most medial boundary. All these divisions are illustrated in Fig. 6 for the finite element model of the cemented, pegged anchorage system. The change in bone mass, calculated for each octant, and its 3 sub-octants, is given by

$$\Delta m = \frac{\sum_{i=1}^{n_V}\left(\rho_i^{final} - \rho_i^{initial}\right) \times V_i}{\sum_{i=1}^{n_V}\rho_i^{initial} \times V_i} \tag{3}$$

where n_V is the number of nodes within the region under analysis, ρ_i^{final} and $\rho_i^{initial}$ are the bone apparent densities at the end and beginning of the bone remodelling simulation, respectively, of node i of the region under analysis, and V_i is the volume associated with the node.

3 Results

The bone remodelling simulations were successfully performed for all finite element models developed considering a healthy and an osteoporotic condition of the bone. On average, the convergence criterion was achieved after 538 (standard deviation (SD): 191, ranging from 310 to 800) iterations for the healthy condition and 423 (SD: 122, ranging from 300 to 608) iterations for the osteoporotic condition. The changes in bone density, with respect to the initial condition, are shown in Figs. 7 and 8 for the healthy and osteoporotic bone, respectively, for both the cemented and cement-

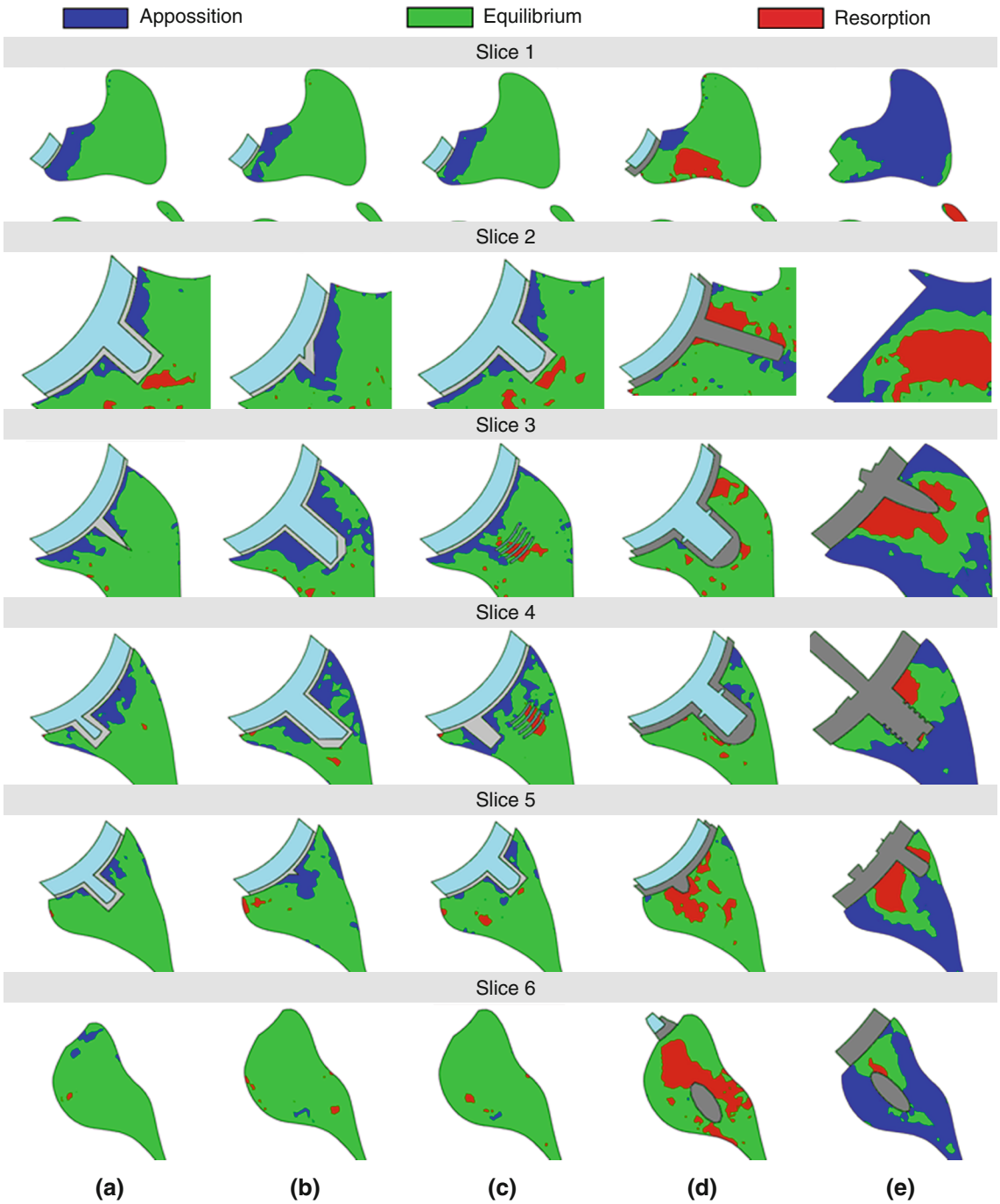

Fig. 7 Change in bone density, with respect to the initial condition, of the healthy bone for **a** the cemented, pegged anchorage system, **b** the cemented, keeled anchorage system, **c** the cemented, anchor pegged anchorage system, **d** the cementless, anatomical implant, and **e** the cementless, reverse implant. The sections of the scapula represented correspond to an inferior to superior view of the slices considered. Equilibrium regions are defined for absolute changes in bone density below 0.072 g/cc

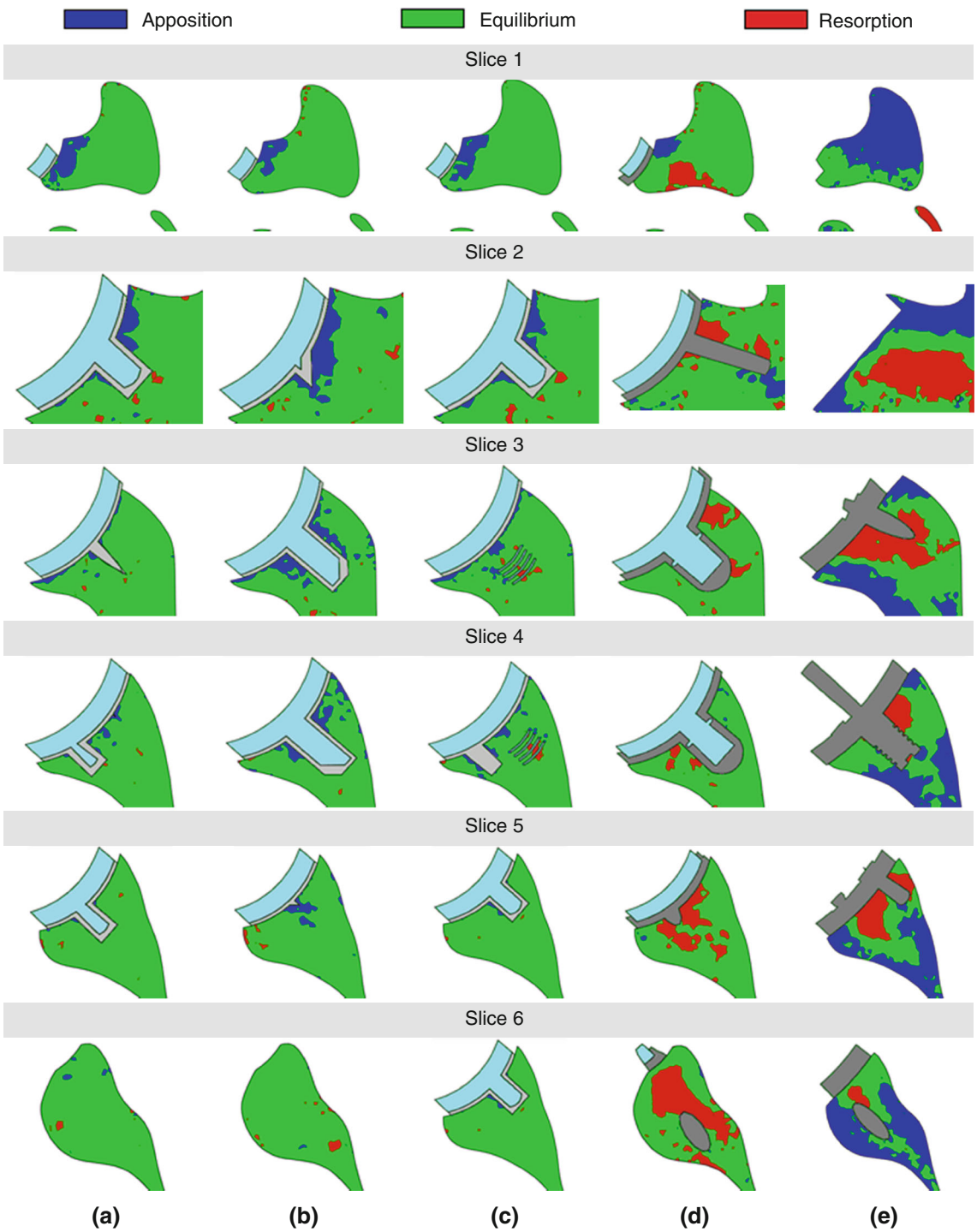

Fig. 8 Change in bone density, with respect to the initial condition, of the osteoporotic bone for **a** the cemented, pegged anchorage system, **b** the cemented, keeled anchorage system, **c** the cemented, anchor pegged anchorage system, **d** the cementless, anatomical implant, and **e** the cementless, reverse implant. The sections of the scapula represented correspond to an inferior to superior view of the slices considered. Equilibrium regions are defined for absolute changes in bone density below 0.072 g/cc

less prostheses, for the slices illustrated in Fig. 5. Figures 9 and 10 quantify the change in bone mass for the 8 octants of the glenoid, and their corresponding sub-octants, for the healthy and osteoporotic bone, respectively. Note that, for the sake of simplicity, the bone adaptation process of the scapula is categorized into bone apposition, equilibrium, and

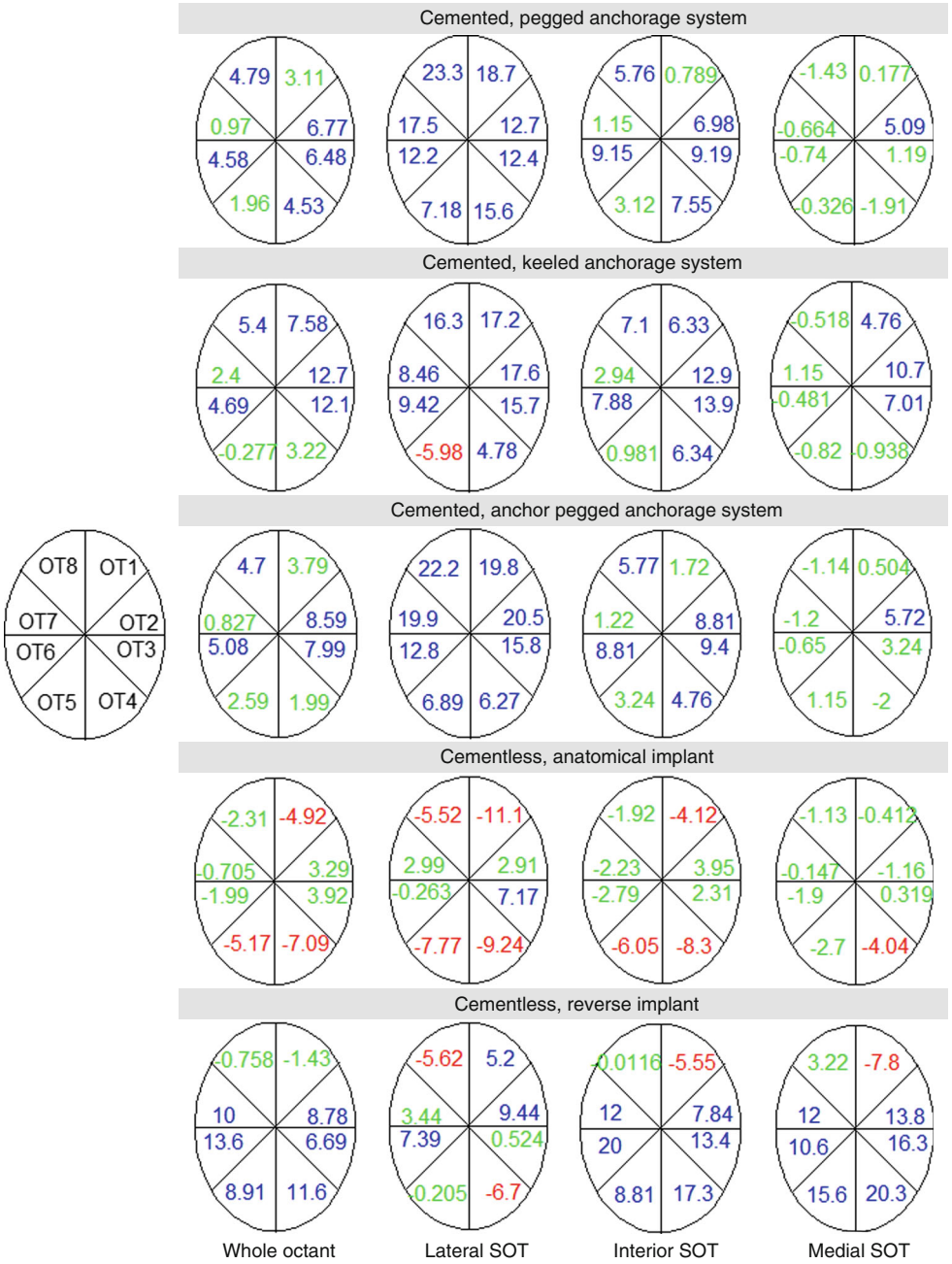

Fig. 9 Change in bone mass, in percentage, with respect to the initial condition, of the healthy bone for the octants, and sub-octants, of the glenoid, described in detail in Fig. 6. The increase, equilibrium, and decrease in bone mass are represented in *blue*, *green*, and *red*, respectively. The equilibrium is defined for absolute changes in bone mass below 4.0 %

bone resorption, being the equilibrium arbitrarily defined for absolute changes in bone density, or bone mass, below 0.072 g/cc, or 4.0 % (Quental et al. 2012a).

3.1 Changes after TSA for healthy bone

The results show that the stress shielding phenomenon is more preponderant for cementless, metal components than for cemented, all-polyethylene components. In fact, despite some small regions being identified in Fig. 7, especially around the cementless central peg of the anchor pegged anchorage system, no significant bone resorption is seen among the cemented, all-polyethylene components. On the other hand, regardless of the anchorage system, all cemented components present several regions of bone apposition, which, in the end, translate into a general gain in bone mass in all octants, and sub-octants, of the glenoid.

The anatomical, cementless component shows significant bone resorption, particularly around the screws, in almost all slices. As a result, there is a decrease of 4.92, 7.09, and 5.17 % in the bone mass of octants OT1, OT4, and OT5, respectively. According to Fig. 9, the major change in bone mass is observed in the lateral sub-octant, i.e. closer to the

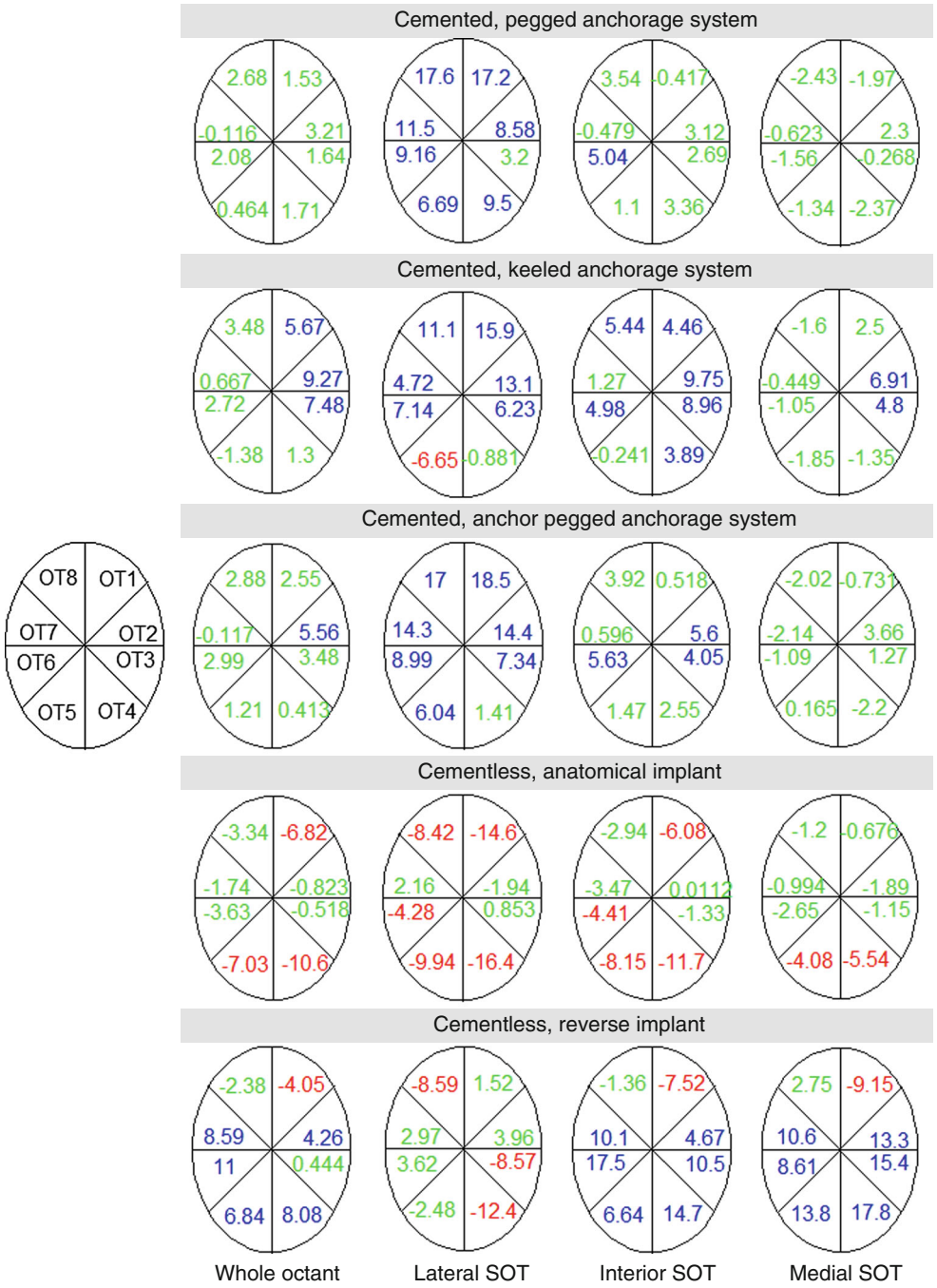

Fig. 10 Change in bone mass, in percentage, with respect to the initial condition, of the osteoporotic bone for the octants, and sub-octants, of the glenoid, described in detail in Fig. 6. The increase, equilibrium, and decrease in bone mass are represented in *blue*, *green*, and *red*, respectively. The equilibrium is defined for absolute changes in bone mass below 4.0 %

interface bone-implant, for which the decrease can be as large as 11.10 %.

The reverse, cementless component shows extensive regions of bone resorption, and apposition, which occur mainly around the screws, and at their edges, respectively. Given the positive, or negligible, change in bone mass in all octants of the glenoid, the rate of bone apposition was clearly superior to that of bone resorption. Nevertheless, the negative effect of the implant on the bone adaptation process must not be neglected as there are several sub-octants showing a significant decrease in bone mass.

3.2 Healthy versus osteoporotic bone

The results obtained for the simulations considering a poorer condition of bone are, qualitatively, similar to those obtained for the healthy condition. In other words, even in such case, the cemented, all-polyethylene components do not appear to be a concerning issue for the bone adaptation process of the scapula, whereas cementless, metal components do. On a quantitative level though, it must be highlighted that the results are generally worse for the osteoporotic bone. In particular, a significant decrease in bone apposition and increase in bone resorption is observed in all octants, and sub-octants, of the glenoid.

4 Discussion

The changes in bone resulting from the insertion of an implant into the scapula have mainly been addressed by stress analyses alone (Stone et al. 1999; Lacroix et al. 2000; Ahir et al. 2004; Gupta et al. 2004a,b). Hence, the bone adaptation process of the scapula is still at an early stage of study. In the light of this, the aim of this study was to evaluate the bone remodelling process of the scapula around cementless and cemented glenoid prostheses and deepen the knowledge of its relevance to the TSA. For that purpose, five finite element models were developed to simulate the replacement of the glenoid by a cemented, all-polyethylene component, with a pegged anchorage system; a cemented, all-polyethylene component, with an anchor pegged anchorage system; a cemented, all-polyethylene component, with a keeled anchorage system; an anatomical, cementless, metal-backed component; and a reverse, cementless, all-metal component. The changes after TSA were qualitatively and quantitatively assessed in terms of bone density for a healthy and an osteoporotic condition of bone. To the author's knowledge, this is the first time that such an extensive bone remodelling analysis is performed for the scapula after TSA. Note that cemented and cementless, and anatomical and reverse, glenoid components are modelled.

Under the assumed modelling conditions, the bone remodelling simulations predicted no significant change in the bone adaptation process of the scapula when this was implanted with a cemented, all-polyethylene component. In other words, the stress shielding phenomenon appears to be negligible in such cases, which confirms what previous studies suggested, i.e. that cemented, all-polyethylene components allow a stress pattern similar to that in the native glenoid (Stone et al. 1999; Lacroix et al. 2000; Gupta et al. 2004b). Regarding the different anchorage systems, the keeled component performed better than both pegged and anchor pegged components, except at the inferior region of the glenoid. The anchor pegged component performed quite similar to the pegged component, but its distinguishing feature, i.e. the cementless central peg, increased the resorption of bone due to the preferential transfer of loads from the cement interface to the thicker cortical wall at the spine of the scapula. Note that such behaviour is not seen in any other peg or keel because they are also surrounded by a mantle of bone cement that allows a more uniform distribution of the loads to the bone.

The results for the cementless, metal components show several regions of significant bone resorption, especially near the bone–implant interface and around the screws, thus supporting the existence of stress shielding. Additionally, as observed in other studies of the shoulder and hip (Cohen and Rushton 1995; Ahir et al. 2004; Quental et al. 2012a; Suárez et al. 2012), the tip of the screws is also associated with a significant increase in bone mass. Given the two additional screws, of smaller length, of the reverse component, placed at the anterior and posterior cortices of the glenoid, the bone growth observed is particularly pronounced in this case. As a result, it must be highlighted that the change in bone mass calculated for the defined octants, and sub-octants, of the glenoid may be underestimating the extent of bone resorption for the reverse component due to the counterbalancing of bone growth. Although predicted for other cementless designs, similar trends were also observed by Ahir et al. (2004); Gupta et al. (2004a) and Suárez et al. (2012).

The bone adaptation process of the scapula considering different conditions for bone showed qualitatively similar results for both osteoporotic and healthy conditions. Nevertheless, it must be noted that the amount of bone resorbed increased significantly in the osteoporotic bone, in opposition to the amount of bone deposited. Therefore, even though the quality of bone does not seem to be as preponderant for the bone adaptation process as in other bones (Ohta et al. 2003; Quental et al. 2012a), this must still not be disregarded. From the numerical point of view, this result evidences that the remodelling parameter κ is not expected to change the qualitative outcome of the bone adaptation process of the scapula. Additionally, it is worth pointing that analyses performed with different values for the remodelling parameter m showed a similar outcome. In particular, for different values of m, some differences in bone apposition and resorption were observed, but the conclusions drawn from the performed study were not affected.

Despite the bone remodelling results being in good agreement with the literature, these must be interpreted within the limitations of the current study. In particular, (1) the bone geometry, bone density, and loading conditions were based on a single, representative, scapula (Schroeder et al. 2001), and (2) all interfaces, bone–implant, cement–implant, and bone–cement, were considered fully bonded, though, in reality, there might be some debonding or relative micromotions, which could change the stresses at these interfaces.

Furthermore, the bone remodelling model applied is not able to reproduce bone resorption due to overload. Considering the same critical stresses assumed by Li et al. (2007), after which bone is resorbed due to overload, the results would not have been affected. Nevertheless, it is relevant to further investigate such resorption mechanism, particularly at the tip of the metallic screws. Another limitation of the current study is concerned with the validation of the bone remodelling simulations. Given the lack of experimental data, these are assumed valid based on the fact that the same methodology successfully simulated the bone adaptation process of the intact scapula (Quental et al. 2013a).

On the opposite side, it is relevant to highlight that the developed finite element models have the advantage of being supported by a multibody system of the upper limb capable of simulating both the anatomical and reverse shoulder anatomies (Quental et al. 2012a, 2013b,c). This feature is particularly important to allow a better definition of the loading condition of the scapula, especially considering the need to appropriately adjust it according to the simulated condition of the shoulder joint. Note that the loads applied to the scapula in the reverse shoulder model were estimated considering an altered shoulder biomechanics, in which the joint centre of rotation was medialized and lowered, and the supraspinatus, infraspinatus, and subscapularis muscles were deactivated.

As far as the bone adaptation process of the scapula is concerned, the results show that cemented, all-polyethylene components are better suited for the replacement of the shoulder joint than cementless, metal components. Nevertheless, it must be highlighted that other biological and mechanical factors, not addressed here, must also be considered to fully evaluate the performance of each component. Other relevant limiting factors that need further research include the mechanical degradation of the cement–implant and bone–cement interfaces in cemented components (Lacroix et al. 2000; Sarah et al. 2010), and bone osteolysis caused by wear in both cemented and cementless components (Strauss et al. 2009; Clement et al. 2010), just to name a few.

Acknowledgments This work was supported by the FCT through the project PTDC/SAU-BEB/103408/2008 and the PhD scholarship SFRH/BD/46311/2008.

References

Ahir SP, Walker PS, Squire-Taylor CJ, Blunn GW, Bayley JIL (2004) Analysis of glenoid fixation for a reversed anatomy fixed-fulcrum shoulder replacement. J Biomech 37(11):1699–1708. doi:10.1016/j.jbiomech.2004.01.031

Bohsali KI, Wirth MA, Rockwood CA Jr (2006) Complications of total shoulder arthroplasty. J Bone Joint Surg Am 88–A(10):2279–2292

Bono JV, Scott RD, Ranawat CS, Turner RH (2005) Revision total knee arthroplasty. Springer, New York

Carter DR, Wong M (2003) Modelling cartilage mechanobiology. Philos Trans R Soc Lond B Biol Sci 358(1437):1461–1471. doi:10.1098/rstb.2003.1346

Christen P, Van Rietbergen B, Lambers FM, Muller R, Ito K (2012) Bone morphology allows estimation of loading history in a murine model of bone adaptation. Biomech Model Mechanobiol 11(3–4):483–492. doi:10.1007/s10237-011-0327-x

Clement ND, Mathur K, Colling R, Stirrat AN (2010) The metal-backed glenoid component in rheumatoid disease: eight- to fourteen-year follow-up. J Should Elbow Surg 19(5):749–756. doi:10.1016/j.jse.2009.11.005

Cohen B, Rushton N (1995) Bone remodelling in the proximal femur after Charnley total hip arthroplasty. J Bone Joint Surg British 77(5):815–819

Farshad M, Gerber C (2010) Reverse total shoulder arthroplasty—from the most to the least common complication. Int orthop 34(8):1075–1082. doi:10.1007/s00264-010-1125-2

Fealy S, Sperling JW, Warren RF, Craig EV (2008) Shoulder arthroplasty: complex issues in the primary and revision setting. Thieme Medical Publishers Inc., New York

Fernandes P, Rodrigues H, Jacobs C (1999) A model of bone adaptation using a global optimisation criterion based on the trajectorial theory of Wolff. Comput Methods Biomech Biomed Eng 2(2):125–138. doi:10.1080/10255849908907982

Folgado J, Fernandes PR, Guedes JM, Rodrigues HC (2004) Evaluation of osteoporotic bone quality by a computational model for bone remodeling. Comput Struct 82(17–19):1381–1388. doi:10.1016/j.compstruc.2004.03.033

Fraldi M, Esposito L, Perrella G, Cutolo A, Cowin SC (2010) Topological optimization in hip prosthesis design. Biomech Model Mechanobiol 9(4):389–402. doi:10.1007/s10237-009-0183-0

Gefen A (2002) Computational simulations of stress shielding and bone resorption around existing and computer-designed orthopaedic screws. Med Biol Eng Comput 40(3):311–322. doi:10.1007/BF02344213

Godest AC, Beaugonin M, Haug E, Taylor M, Gregson PJ (2002) Simulation of a knee joint replacement during a gait cycle using explicit finite element analysis. J Biomech 35(2):267–275

Guedes JM, Kikuchi N (1990) Preprocessing and postprocessing for materials based on the homogenisation method with adaptive finite element methods. Comput Meth Appl Mech Eng 83(2):143–198. doi:10.1016/0045-7825(90)90148-F

Gupta S, Van der Helm FCT, van Keulen F (2004a) The possibilities of uncemented glenoid component—a finite element study. Clin Biomech 19(3):292–302. doi:10.1016/j.clinbiomech.2003.12.002

Gupta S, Van der Helm FCT, van Keulen F (2004) Stress analysis of cemented glenoid prostheses in total shoulder arthroplasty. J Biomech 37(11):1777–1786. doi:10.1016/j.jbiomech.2004.02.001

Hasan SS, Leith JM, Campbell B, Kapil R, Smith KL, Matsen FA 3rd (2002) Characteristics of unsatisfactory shoulder arthroplasties. J Should Elbow Surg 11(5):431–441. doi:10.1067/mse.2002.125806

Hopkins AR, Hansen UN, Amis AA (2005) Finite element models of total shoulder replacement: application of boundary conditions. Comput Methods Biomech Biomed Eng 8(1):39–44. doi:10.1080/10255840512331388155

Huiskes R (1993) Stress shielding and bone resorption in THA: clinical versus computer-simulations studies. Acta Orthop Belg 59(Suppl 1):118–129

Lacroix D, Murphy LA, Prendergast PJ (2000) Three-dimensional finite element analysis of glenoid replacement prostheses: a comparison of keeled and pegged anchorage systems. J Biomech Eng 122(4):430–436. doi:10.1115/1.1286318

Li J, Li H, Shi L, Fok ASL, Ucer C, Devlin H, Horner K, Silikas N (2007) A mathematical model for simulating the bone remodeling process under mechanical stimulus. Dent Mater 23(9):1073–1078. doi:10.1016/j.dental.2006.10.004

Matava MJ, Purcell DB, Rudzki JR (2005) Partial-thickness rotator cuff tears. Am J Sports Med 33(9):1405–1417. doi:10.1077/0363546505280213

Melis B, DeFranco MJ, Laderman A, Barthelemy R, Walch G (2011) The teres minor muscle in rotator cuff tendon tears. Skelet Radiol 40(10):1335–1344. doi:10.1007/s00256-011-1178-3

Nagels J, Stokdijk M, Rozing PM (2003) Stress shielding and bone resorption in shoulder arthroplasty. J Should Elbow Surg 12(1):35–39. doi:10.1067/mse.2003.22

Ohta H, Kobayashi S, Saito N, Nawata M, Horiuchi H, Takaoka K (2003) Sequential changes in periprosthetic bone mineral density following total hip arthroplasty: a 3-year follow-up. J Bone Miner Metab 21(4):229–233. doi:10.1007/s00774-002-0414-2

Pelletier MH, Langdown A, Gillies RM, Sonnabend DH, Walsh WR (2008) Photoelastic comparison of strains in the underlying glenoid with metal-backed and all-polyethylene implants. J Should Elbow Surg 17(5):779–783. doi:10.1016/j.jse.2008.01.138

Poitout DG (2004) Biomechanics and biomaterials in orthopedics. Springer, New York

Quental C, Folgado J, Fernandes PR, Monteiro J (2012a) Bone remodelling analysis of the humerus after a shoulder arthroplasty. Med Eng Phys 34(8):1132–1138. doi:10.1016/j.medengphy.2011.12.001

Quental C, Folgado J, Ambrósio J, Monteiro J (2012b) A multibody biomechanical model of the upper limb including the shoulder girdle. Multibody Syst Dyn 28(1–2):83–108. doi:10.1007/s11044-011-9297-0

Quental C, Folgado J, Fernandes P, Monteiro J (2013a) Subject-specific bone remodelling of the scapula. Comput Methods Biomech Biomed Eng. doi:10.1080/10255842.2012.738198

Quental C, Folgado J, Fernandes P, Monteiro J, (2013b) Critical analysis of musculoskeletal modelling complexity in multibody biomechanical models of the upper limb. Comput Methods Biomech Biomed Eng. doi:10.1080/10255842.2013.845879

Quental C, Folgado J, Ambrósio J, Monteiro J (2013c) Multibody system of the upper limb including a reverse shoulder prosthesis. J Biomech Eng 135(11):111005–111010. doi:10.1115/1.4025325

Rasmussen J, Sorensen AK, Olsen B (2012) Demographic data, clinical outcome and short-term survival after shoulder arthroplasty: 2320 shoulder arthroplasties reported to the Danish shoulder arthroplasty register. J Bone Joint Surg British 94–B(37):36

Santos L, Romeu JC, Canhão H, Fonseca JE, Fernandes PR (2010) A quantitative comparison of a bone remodeling model with dual-energy X-ray absorptiometry and analysis of the inter-individual biological variability of femoral neck T-score. J Biomech 43(16):3150–3155. doi:10.1016/j.jbiomech.2010.07.028

Sarah J, Sanjay G, Sanjay S, Carolyn A, Emery R, Andrew A, Ulrich H (2010) Failure mechanism of the all-polyethylene glenoid implant. J Biomech 43(4):714–719. doi:10.1016/j.jbiomech.2009.10.019

Sharma GB, Debski RE, McMahon PJ, Robertson DD (2010) Effect of glenoid prosthesis design on glenoid bone remodeling: adaptive finite element based simulation. J Biomech 43(9):1653–1659. doi:10.1016/j.jbiomech.2010.03.004

Spitzer V, Ackerman MJ, Scherzinger AL, Whitlock D (1996) The visible human male: a technical report. J Am Med Inf Assoc 3(2):118–130. doi:10.1136/jamia.1996.96236280

Stone KD, Grabowski JJ, Cofield RH, Morrey BF, An KN (1999) Stress analyses of glenoid components in total shoulder arthroplasty. J Should Elbow Surg 8(2):151–158. doi:10.1016/S1058-2746(99)90009-5

Strauss EJ, Roche C, Flurin PH, Wright T, Zuckerman JD (2009) The glenoid in shoulder arthroplasty. J Should Elbow Surg 18(5):819–833. doi:10.1016/j.jse.2009.05.008

Suárez DR, Weinans H, van Keulen F (2012) Bone remodelling around a cementless glenoid component. Biomech Model Mechanobiol 11(6):903–913. doi:10.1007/s10237-011-0360-9

Sundfeldt M, Carlsson LV, Johansson CB, Thomsen P, Gretzer C (2006) Aseptic loosening, not only a question of wear: a review of different theories. Acta Orthop 77(2):177–197. doi:10.1080/17453670610045902

Terrier A, Buchler P, Farron A (2005) Bone-cement interface of the glenoid component: stress analysis for varying cement thickness. Clin Biomech 20(7):710–717. doi:10.1016/j.clinbiomech.2005.03.010

Terrier A, Merlini F, Pioletti DP, Farron A (2009) Total shoulder arthroplasty: downward inclination of the glenoid component to balance supraspinatus deficiency. J Should Elbow Surg 18(3):360–365. doi:10.1016/j.jse.2008.11.008

Von Schroeder HP, Kuiper SD, Botte MJ (2001) Osseous anatomy of the scapula. Clin Orthop Relat Res 383:131–139